Solution of the coupled β functions of the Standard Model and its minimal supersymmetric extension in Python 3

Eduardo Tirado-Félix* and R. J. Hernández-Pinto†

Facultad de Ciencias Físico-Matemáticas, Universidad Autónoma de Sinaloa,
Calzada de las Américas y Calle Universitarios, s/n. Ciudad Universitaria C.P. 80013
Culiacán, Sinaloa, México.

The Standard Model contain three coupling constants α_1, α_2 and α_3 associated to the intern symmetries groups. However, even such constants are named like that, in fact they are not, they are energy dependent functions. The functional form of the evolution satisfy a coupling differential system equations, the coupled β functions. In general these β functions are highly coupled, from this arise the necessity of use numerical methods for the solutions of the problem, because it is not possible obtain it analytically. In this work is used the adaptive Runge-Kutta method for an ordinary differential equations system. The physical motivation of this work arise from the fact that the coupling constants α_1, α_2 and α_3 are associated to the electromagnetic interaction, the weak interaction and the strong interaction, respectively. In the Standard Model, the resulting solution for α_1 and α_2 it is intersected in a point, which can be interpreted that a unification of two fundamental interactions exists. Nevertheless, using the minimal supersymmetric extension of the Standard Model, the three coupling constants intersect in a region, reaching what is known as the Grand Unification.

1 Introduction

Particles and its interactions are tested mainly in high-energy collider machines. The highly precise observables measured in those machines supports strongly the so-called Standard Model (SM). The SM is a unitary gauged quantum field theory of fermions and bosons. It was build over an $SU(3)_c \times SU(2)_L \times U(1)_Y$ which is broken spontaneously to an $SU(3)_c \times U(1)_Q$ theory. The unbroken $SU(3)_c$ gauge group is the responsible of the stability of the proton through the prediction of confinement. On the other hand, the electroweak theory is broken to a symmetry group where the electric charge Q is the conserved quantity in the Noether theorem; the path to this theory is $SU(2)_L \times U(1)_Y \to U(1)_Q$. The mechanism for breaking symmetries turns out to generate masses for all particles in the SM. Furthermore, it gives rise to massless and massive gauge bosons which are responsible of the fundamental interactions.

Symmetries and its implications in nature are then crucial to understand the reactions which takes place, for instance, at the LHC. However, even if the SM can explain mostly all observables, it lacks an explanation the cosmological problems and it starts to manifest some tensions with other highly precise observables as the anomalous magnetic moment of the muon. Many ideas come to play in order to solve

*eduardotirado.fcfm@uas.edu.mx
†roger@uas.edu.mx

those problems such as the inclusion of extra particles and interactions. However, the symmetry principle of the SM is untouched in almost all extensions of the SM. There is one possibility which solves the dark matter problem and maintain the symmetry groups unharmed, supersymmetry. Besides, supersymmetry is a natural extension of the SM since it only enlarges the commutative space-time dimensions to include anti-commutative variables. This brings a new phenomenology in collider experiments and, as it shall be studied in this document, in the mathematical aspects of the theory. One of the most impressive feature is the unification of the three fundamental forces of the SM, the Grand Unification Theories (GUT). A distinctive signatures of the GUT, is the proton decay, the existence of mediating particles between the gauge groups shall bring this phenomena in nature. However, the price to pay is that supersymmetry duplicates the number of particles. There are several experimental constraints to supersymmetric theories, however, there are no doubt that the dark matter problem is still present and supersymmetry shed light to the solution of these unsolved problems in the SM.

In this document, we present the study of the running of the three gauge coupling of the SM and its minimal supersymmetric extension, the so-called Minimal Supersymmetric Standard Model (MSSM). The behaviour of the coupling constants over the energy scale is dictated by a coupled ordinary differential equations, so-called β functions. Therefore, the solution of them cannot be obtained analytically thus it is necessary to solve them numerically. In particular, in this work, we solve the two-loop β functions by implementing the Dormand-Prince method in Python. This document is organized as follows: we start by presenting an overview of the fundamental interactions and the Standard Model; then, we analyze the mathematical properties of the β functions at one-loop accuracy and we exhibit the complexity of the two-loop *beta* functions; then, we present the Dormand-Prince method which belongs to a collection of methods known as *adaptative Runge-Kutta methods*; finally, we present our results and conclusions.

2 Fundamental interactions

The *Philosophiæ naturalis principia mathematica* by Isaac Newton [1] is the first publication where a rigorous explanation of the movement of macroscopic bodies was presented. In this work, it is found three laws of motion which are based on the idea that for changing the movement state of a body they are necessary **forces** that act on it; the nature of these forces are of different kinds such as, friction, viscosity, weight, etc. Hence, the study of fundamental forces has been carried in the forthcoming years, leading to the actual knowledge of the four fundamental interactions: **gravity**, **electromagnetic**, **strong** and **weak**.

The **gravitational interaction** is the most known among the fundamental interactions. It is present between all particles with non vanishing *mass*, it is uniquely attractive and it has an apparently infinite range, therefore, it is responsible of the movement and configuration of the massive objects at large scale in the universe[1]. Nevertheless, the theoretical description of this interaction at the quantum level is one of the most technically challenging. At this level, the isolation of the gravitational force to all others demands new technology in order to measure the interactions of the order of 10^{-30} as in the recent discovery of gravitational waves [2]. However, it is imperative to understand gravity at the microscopic level because, even if its interaction strength is the lowest compared with the other three interactions (see the Table 1), according to General Relativity, the gravitational interaction affects massless particles such as the photon (the particle associated with light). Although, since most experiments are not sensible yet to the gravitational interaction at those scales, its role can be neglected in nuclear processes and high energy collisions without mayor inconveniences.

The **electromagnetic interaction** is manifested between particles with *electric charge*, it can be attractive or repulsive (unlike the gravitational) and it has also an apparently infinite range of action. It conducts almost all phenomena of our daily life (as friction, electricity, chemical reactions and optic ef-

[1] The study of the movement of the astronomical bodies was done many years ago by scientific figures as Kepler, Copernicus, Galileo and Newton.

Interaction	Ratio
Strong	60
Electromagnetic	1
Weak	10^{-4}
Gravitational	10^{-41}

Table 1: Relation between the strength of the four fundamental interactions.* (These calculations are made for two quarks at $3 \times 10^{-17}\ m$) [3]

fects). This interaction is very well known but its concept has been changed over the years. The interpretation of the electric and magnetic phenomena independently has been proven wrong in 1865 when James C. Maxwell was able to unified both phenomena. Furthermore, its quantum implications give rise to the interaction described in the context of *quantum electrodynamics* (QED), the interaction between electrons and photons.

The **weak interaction** is expressed between particles with a property known as *flavor* (also called flavor charge); it has a range less than $10^{-15}\,m$ and is responsible for the *flavor changes* of the elementary particles, it is also responsible for the decay of nuclear particles into lighter particles, and it is crucial to understand some radioactive processes (such as the beta decay).

Finally, the **strong interaction** is experienced between particles with a property known as *colour* (also called colour charge); it is attractive and has an approximately range of $10^{-15}\,m$, so this interaction is not perceptible at scales larger than the atomic nucleus [2]; it is the responsible for the stability of the atomic nucleus and, thereby, of all known matter. The discovery of this interaction came out from the unexpected nature of the atomic nucleus. If the nucleus is formed by protons and neutrons, it was expected the repulsive of the charged particles in the nucleus rendering the nucleus unstable. Latter, it was shown that there is a strongest force that keep protons together, the strong force. This realisation was understood in 1964 with the theory of *quantum chromodynamics* (QCD), proposed by M. Gell-Mann and G. Zweig. [4] [5] [6]

[2] As a reference, the atomic nucleus has a size of the order of $10^{-14}\,m$.

3 Standard Model

As previously mentioned, all forces that govern the phenomena of the universe are the manifestation of the four fundamental interactions. However, what is the mathematical description of all these interactions at the fundamental level? Furthermore, there is still a question about the composition of the matter and how the fundamental building blocks interact among each others. These questions are well explained in the context of the **Standard Model**.

The Standard Model (SM) is the theory that describes the strong, electromagnetic and weak interactions between elementary particles. It postulates the existence of two classes of fundamental spin-1/2 particles that conform matter: quarks and leptons. They can constitute, in the right proportions, any atom and therefore any type of matter in the universe. It also postulates the existence of another group of spin-1 elementary particles, the gauge bosons, that act as carriers of the fundamentals interactions [7]. Additionally, the SM contains a single spin-0 particle, the *Higgs boson*, which is responsible for endowing the particles with mass [8] [9].

Bosons owe their name to the fact that they obey the Bose-Einstein statistics[3] and, as it was mentioned before, gauge bosons are the particles which mediates the fundamental interactions between particles. In nature, experiments have measured the characteristics of four gauge bosons: photons, gluons, $W^{\pm}$ and Z^0. *Photon* is the boson associated to the electromagnetic interaction, the *gluon* is related to the strong interaction and the $W^{\pm}$ *and* Z^0 *bosons* are associated to the weak interaction. As it was stressed in the previous section, up-to-date there is no experimental evidence of the existence of the mediator of the gravitational interaction, the graviton. Experiments dedicated to search for the graviton are not built yet; however, the LHC is continuing on seeking for new particles and interactions and the quantum

[3] Statistics applied to big groups of elementary particles, which are capable to coexist in the same quantum state with the same quantum numbers.

particle of gravity is one of most wanted. Recent LHC searches stands that the graviton must have a mass lower than 6×10^{-32} eV/c^2 [10].

Regarding the SM, it contains the three stronger interactions of all, neglecting the gravitational interaction in all calculations. All known gauge bosons are presented in Table 2.

Name	Symbol	Mass (GeV/c^2)	Electric charge (e)
Photon	γ	0	0
Gluon	g	0	0
$W^{\pm}$ boson	$W^{\pm}$	80.425	± 1
Z^0 boson	Z^0	91.187	0
Higgs boson	H	125.5	0

Table 2: Standard Model Bosons

The spin-1/2 particles are the main constituents of matter. They are considered as structureless particles and they obey the Fermi-Dirac statistics[4], for this reason, they are called **fermions**. This feature allows for layered arrangements of atoms and favouring more complex structures, from atoms to galaxies. Besides, fermions can be classified in **quarks** and **leptons**.

There are six known leptons: electron (e^-), muon (μ^-), tau (τ^-), electron neutrino (ν_e), muon neutrino (ν_μ) and tau neutrino (ν_τ); and six quarks: up (u), down (d), charm (c), strange (s), bottom (b) and top (t), see Table 3. Unlike leptons, quarks have a property called colour and each one can present three colours: red, green and blue.

Due to the strong interaction, quarks create larger structures known as **hadrons**: *baryons* when they are formed by three quarks or three antiquarks, or *mesons* when they are formed as quark-antiquark pairs [5]. The best known hadrons are protons and neutrons, because they formed the nucleus of the atom. The internal structure of the proton is $|\mathbf{uud}\rangle$, that is, two **u**-quarks and one **d**-quark and, the internal quark composition of the neutron is $|\mathbf{udd}\rangle$, it means that it is formed by two **d**-quarks and one **u**-quark [11].

[4]They respect the Pauli exclusion principle, which implies that two fermions cannot be in the same quantum state at the same time

[5]The antiparticle is a particle with the same mass as its corresponding particle but having the opposite charge.

Family	Symbol	Mass (MeV/c^2)	Electric charge (e)
Leptons	e^-	0.511	-1
	ν_e	$< 3 \times 10^{-6}$	0
	μ^-	105.658	-1
	ν_μ	< 0.19	0
	τ^-	1.776.99	-1
	ν_τ	< 18.2	0
Quarks	u	1.5	$+2/3$
	d	4.0	$-1/3$
	c	1.275	$+2/3$
	s	95	$-1/3$
	t	173.210	$+2/3$
	b	4.180	$-1/3$

Table 3: Standard Model Fermions

Although the properties of quarks are well known, free quarks have not been detected yet, that is, they are always confined to hadrons. This explain why quarks can have fractional electric charge and it is also the reason why the range of strong interactions are not beyond the atomic nucleus.

Leptons are the other group of particles that compound matter, the electron being the best understood. It is know that leptons are particles susceptible to weak and electromagnetic interaction, however, it has not been able to determined that they are capable or not to interact with the strong interaction. Another leptons that have been deeply investigated are neutrinos because they have a very small mass (in the beginning it was thought that they were massless) and almost they do not interact with matter. These particles can reveal the complete image of universe from the moment it was formed (the Big Bang), since these *remnants neutrinos* are still founds in the farthest regions of the horizon of space.

As it was shown in the Table 2 and Table 3, the mass of the particles is expressed in units of energy over c^2 (c is the speed of light in vacuum). We can use these units by virtue of the equation that Einstein derive in the Special Relativity theory, $E = mc^2$ [6]

[6]This equation is a particular case of the equation $E^2 = (pc)^2 + (mc^2)^2$, applied to particles at rest.

[12]. This equation gives a relation between the rest mass and energy of a body, rearranging in such a way that $m = \frac{E}{c^2}$. Electron-volts (eV) units are used instead of Joules because the eV definition is more suited to elementary particles scale than the Joules definition. 1 eV is the energy acquired by an electron moving between two points that are at an electrical-potential of $1\,V$; on the other hand, $1\,J$ is the work done by a constant force of $1\,N$ moving a body a distance of $1\,m$. The relation between both units is $1\ eV = 1.602 \times 10^{-19}\ J$.

4 Coupling constants, beta functions and gauge couplings

So far, we have stated that the fundamental interactions have different intensities, so it is useful to use parameters that show a value that allow us to know and compare the magnitudes of each interaction. Here is where the SM make use of the *coupling constants*.

The **coupling constants** of the fundamental interactions are dimensionless constants that tell us the strength of each interaction. The approximate values of each coupling constant are shown in Table 4. It should be clarified that, for the purposes of this work, the notation α_1, α_2 and α_3 will be used for the coupling constant of the electromagnetic, weak and strong interaction, respectively. Among these coupling constants, the best known is α_1, which is called *fine structure constant* and it is assigned the symbol α. This constant is related to the electromagnetic interaction that appears in various physical processes and it was introduced in 1916 by Arnold Sommerfeld while he was working in the atomic model of Bohr. In his work, Sommerfeld used α to quantify the gap in the fine structure of the spectral lines of the hydrogen atom [13].

As specified in Table 4, the values of a given coupling constant is set at the energy of 1 GeV. Why it is specified this value if they are called *constants*? This value is set because these coupling *constants* are not really constant in energy. The coupling constants are dependent functions on the energy scale at which one is performing a calculation, thus at a bigger energy scale the given values are not the same. To be able to know the behaviour of the coupling constants, they are used a set of differential equations known as the β *functions*.

Interaction	Symbol	Value
Strong	α_3	1
Electromagnetic	α_1	1/137
Weak	α_2	10^{-6}
Gravitational	α_g	10^{-39}

Table 4: Aproximate values of the coupling constants of the fundamental interactions (at 1 GeV).

The β **functions** are differential functions that describe the evolution of some parameters g, known as **gauge coupling**, according to the energy scale Q. Gauge couplings are related to the SM gauge groups, $SU(3)_c \times SU(2)_L \times U(1)_Y$, namely, g_3, g_2 and g_1. The importance of these parameters is that they are used to series expand expression in pertubative calculations [7]. In this aim, the expressions obtained for β functions are known as a series expansion in those parameters. As mentioned before, the gravitational interaction is not considered in the Standard Model, therefore we will only have β functions for the others three interactions.

At second order in perturbation theory, so called *two-loops*[8], gauge couplings g_1, g_2 and g_3 evolve according to differential equations of the form,

$$\frac{dg_l}{dt} \equiv \beta_l(g) = -b_l \frac{g_l^3}{16\pi^2} - \sum_{k=1}^{3} b_{kl} \frac{g_k^2 g_l^3}{(16\pi^2)^2}, \qquad (1)$$

where $t = \log(Q/Q_0)$ and $l = 1,\ 2,\ 3$. The Q_0 term is an arbitrary energy scale that is chosen to fix the experimental measurements. For the purpose of this work it is used $Q_0 = 1$ GeV. It is also important to mention that in Eq. (1) is omitted a last term that

[7] Perturbation theory is a collection of approximate schemes to describe complex quantum systems in terms of simpler ones.

[8] The perturbation theory is based in the use of a power series solution and the contributions of this series are given by the number of loops. At greater number of loops the series approximate more to the real solution.

represents Yukawa couplings contributions [14]. This approximation can be used as this step because its contribution is very small with respect to the contributions presented in Eq. (1). Furthermore, if Yukawa terms are added, one needs to add the evolution of them according to the so-called anomalous dimensions at two-loops, which is out of the reach of this work.

It is worth appreciating that Eq. (1) has the most general two-loop contribution to the β function. It can be used to describe the SM running of the gauge couplings, or the running of gauge coupling in different models, as it shall be used in the minimal supersymmetric extension of the SM.

In the SM, the b_l coefficients are given by,

$$\begin{aligned} b_1 &= -\frac{4}{3}n_g - \frac{1}{10}, \\ b_2 &= \frac{22}{3} - \frac{4}{3}n_g - \frac{1}{6}, \\ b_3 &= 11 - \frac{4}{3}n_g, \end{aligned} \tag{2}$$

where n_g is the number of generations or families. Experimental results indicates that the most consistent value is $n_g = 3$. In addition, b_{kl} coefficients are given by the entries of the matrix,

$$\begin{aligned} (b_{kl}) = &\begin{pmatrix} 0 & 0 & 0 \\ 0 & \frac{136}{3} & 0 \\ 0 & 0 & 102 \end{pmatrix} - n_g \begin{pmatrix} \frac{19}{15} & \frac{1}{5} & \frac{11}{30} \\ \frac{3}{5} & \frac{49}{3} & \frac{3}{2} \\ \frac{44}{15} & 4 & \frac{76}{3} \end{pmatrix} \\ &- \begin{pmatrix} \frac{9}{50} & \frac{3}{10} & 0 \\ \frac{9}{10} & \frac{13}{3} & 0 \\ 0 & 0 & 0 \end{pmatrix}. \end{aligned} \tag{3}$$

On the other hand, these gauge couplings are closely related to the coupling constants, which satisfy the following equation,

$$\alpha_i = \frac{g_i^2}{4\pi}, \qquad \text{para} \;\; i = 1, 2, 3. \tag{4}$$

Therefore, once the evolution of the gauge couplings with respect energy is obtained, we will be able to know how the coupling constants evolves with energy.

At first order in perturbation theory, the so-called *one-loop* calculation, β functions only takes into consideration the term proportional to b_l. This simplification make the calculation more simple than it can be solved analytically. In this scenario, the system of differential equations are given by,

$$\frac{dg_l}{dt} = -b_l \frac{g_l^3}{16\pi^2}, \qquad \text{para} \;\; l = 1, 2, 3, \tag{5}$$

where the coefficients b_l are the same as those in Eqs. (2). This system has the β functions decoupled, however, its solution shall be less accurate than the two-loop calculation. Nevertheless, it is important to highlight its analytic behaviour. At an arbitrary energy scale $Q = M$ and with initial conditions $g_l(M)$, for $l = 1, 2, 3$, the solution of Eq (5) is found to be,

$$g_l(Q) = \frac{1}{\sqrt{[g_l(M)]^{-2} + \left(\frac{b_l}{8\pi^2}\right) \ln\left(\frac{Q}{M}\right)}}, \quad l = 1, 2, 3. \tag{6}$$

In this way, the coupling constants are:

$$\alpha_l(Q) = \frac{1}{4\pi\left([g_l(M)]^{-2} + \left(\frac{b_l}{8\pi^2}\right) \ln\left(\frac{Q}{M}\right)\right)} \qquad l = 1, 2, 3. \tag{7}$$

5 Unification of fundamental interactions

Throughout history, we have learnt that the study of different phenomena converged to the analysis of the four fundamental interactions. It seems that, under a particular point of view, all kind of forces can be understood as a manifestation of one of these forces. This line of thinking give rise to the *unification* concept. The best example of unification was the one happened between the electric and magnetic phenomena. The unification of these two aspects into a single concept is rigorously explained in Maxwell's equations. Therefore, it is natural to pursue the answer of

the question: are the four fundamental interactions really different or are they simply a consequence of an unknown interaction?

The seek to the answer to this question take us back to the period of 1960-1970, 100 years after the unification of electromagnetism. The weak theory was observed primarily by experiments and the main theoretical contributions were made by Steven Weinberg [15], Abdus Salam [16] and Sheldon Glashow [17], all of them working independently. The agreement between theory and the experimental data needed, from the theory side, the inclusion of the electromagnetic interaction meaning that, this interaction necessarily must be be unified with the weak interaction in a single interaction, so called *electroweak interaction*.

The path to unification implies that if weak and electromagnetic interactions are of the same order, then the mass of the Z^0 boson is negligible and is *on equal footing* with the photon [18]. Although, the problem is that it is known that the mass of the Z^0 boson is not insignificant and, in fact, it is the third most massive particle in the SM; moreover, as seen in Table 4, at the scale energy of 1 GeV the interactions do not have the same intensity. The explanation to these facts can be found in the unification of the electroweak theory through the $SU(2) \times U(1)_Y$ gauge groups. Once the electromagnetic and weak interactions were unified, the next step on the list would be try to unified the other interaction that is within the SM: the strong interaction. This theoretical unification of the three interactions it is known as the **Grand Unification**. Unfortunately, in the context of the SM this unification do not occur, but it is still possible to achieve within the framework of *supersymmetry*.

Supersymmetry is a theory, unverified experimentally, that describes a symmetry between bosons and fermions. Both quantum states are related through supersymmetric transformation, which changes a bosonic state into a fermionic state and vice versa. Besides, each particle is associated to a supersymmetric partner that differs in spin by a half-integer [19]. Within the supersymmetric theories, there is one known as **Minimal Supersymmetric Standard Model** (MSSM), which owes its name to the fact that it contains the smallest number of new particle states and new interactions consistent with phenomenology. Within the MSSM, the Grand Unification is possible at energy scales of the order of 10^{16} GeV. The estimated scale is given by the evolution of the β functions.

The functional form of the associated β functions expressed in Eq. (1) and Eq. (5) are the same for the MSSM, with the only modification of the coefficients b_l and b_{kl} of Eq. (2) and Eq. (3). In general, the coefficients at one-loop can be obtained by investigating the mathematical structure of the gauge groups. Considering any $SU(N)$ gauged QFT or SUSY QFT, the b_l coefficients are given by [14],

$$b_l = \frac{11}{3} C_2(G) - \frac{4}{3} \kappa S_2(F) - \frac{1}{6} \eta S_2(S) , \qquad (8)$$

where $C_2(G)$ is the quadric Casimir invariant acting over gauge fields, $S_2(F)$ and $S_2(S)$ are the Dynkin indices over fermion and scalar field representations respectively, $\kappa = \{\frac{1}{2}, 1\}$ for Dirac and Weyl fermions and $\eta = 1, 2$ for real and complex scalar fields respectively. In the MSSM, the numerical values of these coefficients are [20]:

$$b_1 = -\frac{33}{5}, \qquad b_2 = -1, \qquad b_3 = 3, \qquad (9)$$

and, the two-loop contributions are given by,

$$(b_{kl}) = - \begin{pmatrix} \frac{199}{25} & \frac{27}{5} & \frac{88}{5} \\ \frac{9}{5} & 25 & 24 \\ \frac{11}{5} & 9 & 14 \end{pmatrix} . \qquad (10)$$

It is possible to appreciate that the differentials equations associated to the β functions are functionally the same, but with different coefficients, so it is of interest for this work to find a way to solve them numerically, and to show the Grand Unification in present in supersymmetric theories such as the MSSM. In the next section, we present the method used in this work to solve the coupled differential equations for a large range of energy scales, the Dormand-Prince method.

6 The Dormand-Prince method

For the solution of the system of differential equations given by Eq. (1), for the SM (coefficientes of Eqs. (2), (2.2), (2.3) and (3)) and the MSSM (coefficients of Eqs. (9) and (10)), we performed the **Dormand-Prince method**, which is part of a collection of methods to solve ordinary differential equations with initial conditions, known as **adaptive Runge-Kutta methods**. In the following, we recall the ideas behind the method.

Let us start with an ordinary differential equation with initial condition,

$$y' = f(t, y), \qquad y(t_0) = y_0. \tag{11}$$

The expression of the explicit Runge-Kutta method of order p comprise a weighted average of values of $f(t, y)$ taken at different points in the interval $t_n \leq t \leq t_{n+1}$, given a number s of stages, is expressed by,

$$y(t + h) = y(t) + \sum_{l=1}^{s} d_l k_l, \tag{12}$$

where the value h [9] represents the spacing over the values of t; and,

$$k_1 = hf(t, y), \tag{13}$$

$$k_i = hf\left(t + c_i h, y + h\sum_{j=1}^{i} a_{i,j} k_j\right), \quad i = 2, 3, ..., s\,. \tag{14}$$

The coefficients $a_{i,j}$, d_l and c_i vary according to the method used, but in order for the method to be consistent it must satisfies that

$$\sum_{l=1}^{s} d_l = 1\,. \tag{15}$$

In addition, to obtain a Runge-Kutta method of order p (hence, to obtain an overall truncation error of $\mathcal{O}(h^p)$), the relation,

$$\sum_{j=1}^{i-1} a_{i,j} = c_i \text{ for } i = 2, 3, ..., s\,, \tag{16}$$

must be fulfilled [21].

This method is also useful for a system of m first order ordinary differential equations,

$$y_i' = f_i(t, y_1, y_2, ..., y_m), \qquad y_i(t_0) = y_{0i}, \tag{17}$$

for $i = 1, 2, ..., m$. Hence, it is simpler to write the formalism in in vector form. Defyning

$$\begin{aligned}
\mathbf{y} &= (y_1, y_2, ..., y_m),\\
\mathbf{f} &= (y_1', y_2', ..., y_m'),\\
\mathbf{k}_1 &= h\mathbf{f},\\
\mathbf{k}_i &= h\mathbf{f}\left(t + c_i h, \mathbf{y} + h\sum_{j=1}^{i} a_{i,j}\mathbf{k}_j\right), \quad i = 2, 3, ..., s
\end{aligned} \tag{18}$$

therefore,

$$\mathbf{y}(t + h) = \mathbf{y}(t) + \sum_{l=1}^{s} d_l \mathbf{k}_l. \tag{19}$$

Adaptive Runge-Kutta methods estimate the truncation error in each step of the solution and automatically adjust the step size to keep the error within the limits specified by the user. These techniques use two explicit Runge-Kutta methods: one of order p and another of order $p + 1$, in order to estimate the truncation error used in both formulas and therefore, to make the appropriate adjustment of h. The *calibration* of the step size is extremely important because it could find solutions in faster computation time and, therefore, there is no delay in finding the appropriate step size.

The Dormand-Prince method uses Runge-Kutta methods of order 4 and 5 with a total of 7 stages, so the system of equations are,

$$\begin{aligned}
\mathbf{y}_4(t + h) &= \mathbf{y}(t) + \sum_{l=1}^{7} d_{4l} \mathbf{k}_l,\\
\mathbf{y}_5(t + h) &= \mathbf{y}(t) + \sum_{l=1}^{s} d_{5l} \mathbf{k}_l,
\end{aligned} \tag{20}$$

[9] h is also often called *size step* or simply *step*.

l	d_{4l}	d_{5l}	c_l
1	$\frac{5179}{57600}$	$\frac{35}{384}$	-
2	0	0	$\frac{1}{5}$
3	$\frac{7571}{16695}$	$\frac{500}{1113}$	$\frac{3}{10}$
4	$\frac{393}{640}$	$\frac{125}{192}$	$\frac{4}{5}$
5	$-\frac{92097}{339200}$	$-\frac{2187}{6784}$	$\frac{8}{9}$
6	$\frac{187}{2100}$	$\frac{11}{84}$	1
7	$\frac{1}{40}$	0	1

Table 5: Coefficients of the Dormand-Prince method

with

$$\mathbf{k}_1 = h\mathbf{f}(t, \mathbf{y}),$$
$$\mathbf{k}_i = h\mathbf{f}\left(t + c_i h, \mathbf{y} + h\sum_{j=1}^{7} a_{i,j}\mathbf{k}_j\right), \quad i = 2, 3, ..., 7. \tag{21}$$

The coefficients of the method are given in Table 5 and the matrix a is,

$$a = \begin{pmatrix} 0 & 0 & 0 & 0 & 0 & 0 \\ \frac{1}{5} & 0 & 0 & 0 & 0 & 0 \\ \frac{3}{40} & \frac{9}{40} & 0 & 0 & 0 & 0 \\ \frac{44}{45} & -\frac{56}{15} & \frac{32}{9} & 0 & 0 & 0 \\ \frac{19372}{6561} & -\frac{25360}{2187} & \frac{64448}{6561} & -\frac{212}{729} & 0 & 0 \\ \frac{9017}{3168} & -\frac{355}{33} & \frac{46732}{5247} & \frac{49}{176} & -\frac{5103}{18656} & 0 \\ \frac{35}{384} & 0 & \frac{500}{1113} & \frac{125}{192} & -\frac{2187}{6784} & \frac{11}{88} \end{pmatrix}. \tag{22}$$

Thus, we have that the formula of order 4 is used to implicitly estimate the truncation error, so that the truncation error is given by:

$$\mathbf{E}(h) = \mathbf{y}_5(t+h) - \mathbf{y}_4(t+h) = \sum_{l=1}^{7}(d_{5l} - d_{4l})\mathbf{k}_l. \tag{23}$$

Note that this error is a vector where each component E_i corresponds to the truncation error of the y_i variables, so we have to choose a way to measure a value of the error $e(h)$. The choice employed is to use *mean squared error* to consider all the variables. Thus, in this work, we decide to use the step size is,

$$e(h) = \sqrt{\frac{1}{3}\sum_{i=1}^{3} E_i^2}. \tag{24}$$

Error control is obtained by adjusting the increment of h such that the error $e(h)$ is approximately equal to a preset tolerance ϵ. Since the method of order 4 has a local truncation error of $\mathcal{O}(h^5)$, we have that,

$$\frac{e(h_1)}{e(h_2)} \approx \left(\frac{h_1}{h_2}\right)^5. \tag{25}$$

In this way, once the step h_1 and the error $e(h_1)$ are obtained, the step h_2 obtained with a specific tolerance ϵ is:

$$h_2 \approx h_1\left[\frac{\epsilon}{e(h_1)}\right]^{\frac{1}{5}}. \tag{26}$$

If $\epsilon \geq e(h_1)$, the truncation error is good enough so the calculation is accepted and the step h_2 is taken for the next point (here is where the step increases). On the other hand, if $\epsilon < e(h_1)$, the error is out of the accepted range, so this step is repeated with h_2, which leads to a reduction of the step in order to obtain a better result [22].

In this work, we have that the initial conditions of the gauge couplings are given at the energy of the top quark mass, $m_t = 173.37$ GeV [23],

$$g_1(m_t) = \left(\sqrt{\frac{5}{3}}\right)(0.3594),$$
$$g_2(m_t) = 0.64654,$$
$$g_3(m_t) = 1.16666. \tag{27}$$

Hence, with this initial conditions, the solutions of Eq. (5) take the values $M = m_t$ and $g_l(m_t)$. In the

case of Eq. (1) we have a system of three coupled differential equations,

$$\begin{aligned} g_1' &= f_1\left(Q, g_1, g_2, g_3\right), \\ g_2' &= f_2\left(Q, g_1, g_2, g_3\right), \\ g_3' &= f_3\left(Q, g_1, g_2, g_3\right), \end{aligned} \tag{28}$$

and where the tolerance has a value of $\varepsilon = 10^{-10}$. Finally, it is important to make three clarifications about the code used for the Dormand-Prince method,

i) The relation found between the steps h_1 and h_2 is based on an approximation, therefore, it is good to have a small safety margin, so the relation used is,

$$h_2 = 0.9\, h_1 \left(\frac{\epsilon}{e(h_1)}\right)^{\frac{1}{5}}. \tag{29}$$

ii) In adition, in order to avoid a very large step, it is implemented the restriction,

$$0.1 \leq \frac{h_2}{h_1} \leq 10 \tag{30}$$

iii) One of the advantages of the Dormand-Prince method is that it is only necessary to compute directly $\mathbf{k}_1$ once, since it is satisfied that: if the $n-$th computation of the step is accepted,

$$(\mathbf{k}_1)_{n+1} = \frac{h_{n+1}}{h_n}(\mathbf{k}_7)_n\,; \tag{31}$$

and if the $n-$th computation is not accepted,

$$(\mathbf{k}_1)_{n+1} = \frac{h_{n+1}}{h_n}(\mathbf{k}_1)_n\,. \tag{32}$$

iv) Finally, since this method chooses the step size it considers optimal, the energies where the value of the coupling constants are calculated will most likely to be different for different models; for instance, for the SM and the MSSM. This is why we use the function *interp1d* of the interpolation module *scipy.interpolate* of the library *SciPy*, in order to perform the calculations of the coupling constants at common energies between models.

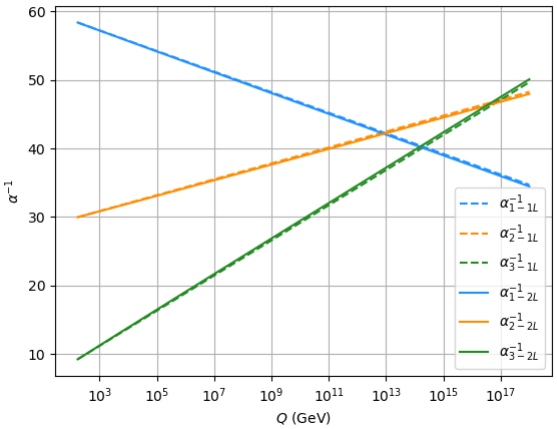

Figure 1: Evolution of the coupling constants in SM at two loops. The values of α_1^{-1} (blue), α_2^{-1} (orange) and α_3^{-1} (green) are those corresponding to the electromagnetic, weak and strong interaction, respectively. The continuous lines are those corresponding to the two loops solution, α_{i-2L}^{-1}, and the dashed ones to one loop solutions, α_{i-1L}^{-1}.

7 Results

The numerical solutions of the β functions of SM at one (Eq. (5)) and two loops (Eq. (1)) using the Dormand-Prince method are plotted in Fig. 1. Since coupling constants have values between 0 and 1, it is common to present, for a better visualization of the solutions, the inverse of each coupling constant, α_i^{-1}.

From these results we have that the coupling constant of the electromagnetic interaction increases and the coupling constants of the weak and strong interaction decrease as we increase the energy scale. Therefore, the intensity of these interactions is affected differently as the energy varies. Moreover, it is obtained that the coupling constants reach in pairs the same values at some energy scales, which leads us to conjecture that at such energy scale, where the intersection takes place, a unification of the corresponding fundamental interactions could occur.

Focusing on the solutions, it can be noticed an apparent discrepancy of these with respect to the val-

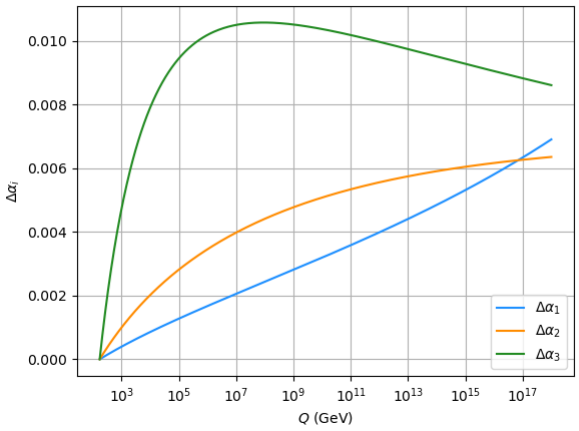

Figure 2: Comparison between coupling constants of SM at one and two loops. The values of $\Delta\alpha_1$ (blue), $\Delta\alpha_2$ (orange) and $\Delta\alpha_3$ (green) are those corresponding to the electromagnetic, weak and strong interaction, respectively.

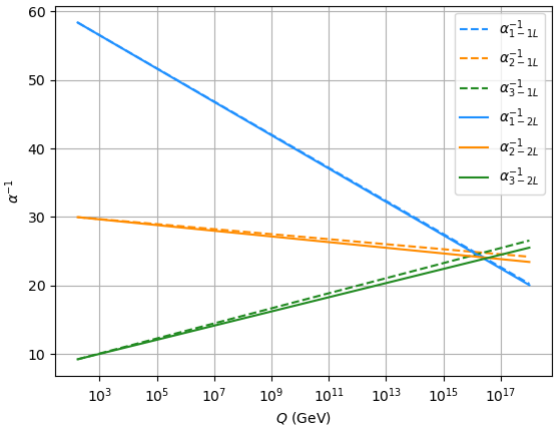

Figure 3: Evolution of the coupling constants in MSSM at two loops. The values of α_1^{-1} (blue), α_2^{-1} (orange) and α_3^{-1} (green) are those corresponding to the electromagnetic, weak and strong interaction, respectively. The continuous lines are those corresponding to the two loops solution, α_{i-2L}^{-1}, and the dashed ones to one loop solutions, α_{i-1L}^{-1}.

ues presented in Table 4, since at a low energy scales they do not seem to coincide; although this is due to the fact that the differential equations solved in this work, the β functions, are a smaller set of differential equations from the so called *Renormalization Group Equations*. This does not detract from the validity of the result, since the initial conditions are obtained experimentally and the evolution of the coupling constants is dictated by the differential equations employed in this work. Furthermore, it is important to highlight that the solution of the β functions can give a glimpse of the unification patern of the fundamental forces.

We present in Fig. 1, the solution of the β functions at one- and two-loops, α_{i-1L} and α_{i-2L} respectively, where $i = 1, 2, 3$ for the different gauge groups of the SM. It is important to point out that both solutions present the same behaviour with small differences. To quantify this difference between solutions we obtain an *error* calculated according to equation,

$$\Delta\alpha_i = \left| \frac{\alpha_{i-2L} - \alpha_{i-1L}}{\alpha_{i-2L}} \right| , \qquad i = 1, 2, 3. \tag{33}$$

In Fig 2, we compute the variations of the two-loop computation with respect to the one-loop scenario. We observe that the differences are very small, and they are in the range of 0 to 1 %. We remark the largest deviation are in the strong coupling constant, it means that the in full calculation large errors can be expected from this interaction at energies around 10^7 GeV. Let us remark that even if the differences could be small, they are not negligeable at large energies, since small contributions could represent a considerable change in the value of the *total cross section*[10], σ, which theoretically can be represented as a series expansion on the parameters α_i. It is well known that in QCD, large contributions could emerge when the perturbative expansion of the theory is considered. In particular, following the perturbation theory in QCD, the total cross section takes

[10]The cross section is a measure of the probability that a specific process takes place at high energetic collisions.

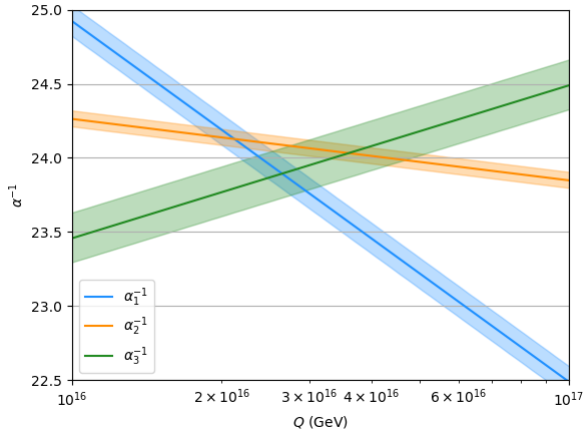

Figure 4: Running of β functions at two-loops near the unification point.

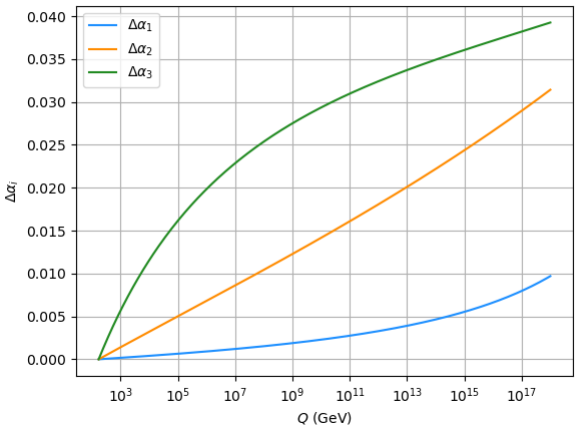

Figure 5: Comparison between coupling constants of MSSM at one and two loops. The values of $\Delta\alpha_1$ (blue), $\Delta\alpha_2$ (orange) and $\Delta\alpha_3$ (green) are those corresponding to the electromagnetic, weak and strong interaction, respectively.

the form,

$$\sigma = \sigma_0 + \alpha_S\sigma_1 + \alpha_S^2\sigma_2 + \cdots = \sum_{n=0}^{\infty} \alpha_S^n \sigma_n, \qquad (34)$$

where the σ_n terms are the calculations of the cross section at a fixed order and $\alpha_S \equiv \alpha_3$. Therefore, it means that small changes in the coupling constants can be compensated as the number of loops are increased in the cross section at higher orders.

We turn our attention to the MSSM scenario. The solution of the β functions of MSSM at one- and two-loops are plotted in Fig. 3. In this case we have that the intensity of the electromagnetic and strong interaction follow the same behaviour as in the SM scheme as the energy scale increases; they only change the slope of the straight lines. A different behaviour is observed in the corresponding coupling to the $SU(2)$ gauge group increases as the energy scale increases. It can be also be realized that, thanks to supersymmetric extension of the SM, the interactions show a unification at an energy scale of about 10^{16} GeV. In fact, it is important to notice that this unification is not exactly at one point but the three coupling constants are contained in a compact enough region to be considered valid. This fact can be noticed in Fig. 4, where we have taken experimental errors at M_Z into consideration. This allow us, in the case of the existence of supersymmetric theories, to undestand the path to Grand Unification and, therefore, to understand that the electromagnetic, weak and strong interactions could be a manifestations of a single fundamental interaction.

Despite the theoretical achievement of the Grand Unification, it is important to mention that, at the date of publication of this work, experimental evidence of supersymmetry has not been found. Regardless of the absence of experimental evidence, the Large Hadron Collider (LHC) is continuously seeking to solve the puzzles of nature, such as dark matter or the dynamical generation of electroweak symmetry breaking, among other, and the existence of MSSM could explain some of these issues in the SM. Then, unceasing efforts from the experimental and theoretical analysis maintain supersymmetry on the market to be proven in future colliders at higher energies.

Similarly to the SM, the MSSM values for the coupling constants differ slightly between the values at one- and two- loops. From this deviation it was cal-

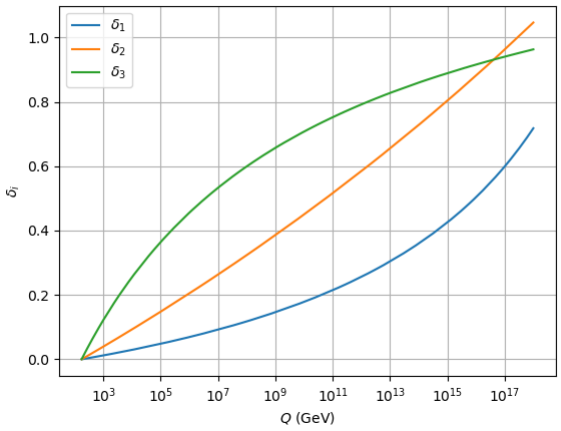

Figure 6: Comparison between coupling constants of the SM and MSSM at two loops. The values of δ_1 (blue), δ_2 (orange) and δ_3 (green) are those corresponding to the electromagnetic, weak and strong interaction, respectively.

culated an error associated to each constant given by Eq. (33) and the results of this error are shown in Fig. 5. In this case, the errors between coupling constants at one- and two-loops are in the range of 0 to 4 %. They represent still very small deviations but not negligible. These errors follow a similar behaviour to the SM solutions, in particular, regarding to the fact that the interaction that expresses large contributions at two-loops is the strong interaction, while the electromagnetic interaction is the least affected.

Finally, it can be seen in Fig. 1 and in Fig. 3 that while in the SM the fundamental interactions appear to have unifications only by pairs and at different energy scales, in the MSSM is presented the unification of all of them at a similar energy scale. In order to appreciate how large the coupling constants differ from one to another model, we calculate the relative *error* to the coupling constant α_i at two loops, taking the SM values as a reference. Thus, these errors are given by,

$$\delta_i = \left| \frac{\alpha_{i-SM} - \alpha_{i-MSSM}}{\alpha_{i-SM}} \right|, \qquad i = 1, 2, 3. \tag{35}$$

Deviations of the MSSM and SM β functions are plotted in Fig. 6. From this figure we found that the deviations between models are in the range of 0 to 100 %. As it is expected from Fig. 1 and Fig. 3, the α_2 presents the largest numerical difference due to the fact that the slope changes from positive to negative; this behavior is not present in α_1 and α_3. Noteworthy, α_3 is not the most different among the three coupling constant, however, the behaviour of it at large energies is very distinct from the SM behavior, of the order of 10% at 10^3 GeV and 40% at around 10^5 GeV. These differences between models are indeed quite large although they describe the same behaviour as the comparison of Fig 2 and Fig. 5, which can be interpreted as the QCD theory is the most sensible to bring light to supersymmetry at the LHC energies or in the FCC [24–27].

8 Conclusions

Numerical methods are a fundamental piece in scientific progress, thanks to them we can solve problems that can not be solvable analytically but we can find an approximate solution. In this work, we have used numerical methods to analyse the coupled β functions at two-loops for the SM and the MSSM. Analitically, we have computed the solution of the one-loop β functions since in this scenario the solution can be solved exactly. However, at two-loops the set of differential equations correspond to a system of coupled differential equations whose terms are not linear. In this work, we have implemented the Dormand-Prince method in Python 3 since the range in which we want to solve the problem is very large, making it practically impossible to solve it with an explicit Runge-Kutta method causing, for instance, that the problem would require a lot of computation time and would consume considerably RAM memory.

The numerical calculations of the solutions of the β functions with loop corrections bring us closer, by means of the perturbation theory, to the real solution of the coupling constants and therefore, to an accurate prediction of the cross section. In addition, since future colliders are planned to reach the precision frontier, it is imperative to known numerical meth-

ods to compute our theoretical predictions. In addition, the β functions solved in this work represents a set of differential equations that must be solved in order to have a better understanding of physics at scales that we have not reached yet. The renormalization group equations at two-loops in the SM and the MSSM would represent the next step in order to test the capabilities of the code developed in this work. Since the main purpose of this study is the conceptual challenge of the Grand Unification of fundamental forces, we have neglected Yukawa terms in the differential equations.

The numerical calculations allow us to test the results such as the Grand Unification scenario and the discrepancies among both models. In particular, we find that in the SM, the maximum deviations for the coupling constants are about 0.7% for α_1, 0.625% for α_2 and 1.25% for α_3 between one and two loop calculation. On the other hand, the MSSM has maximum deviations between one and two loop of the order of 1% for α_1, 3.25% for α_2 and 3.95% for α_3. In addition, the numerical solution of the coupled β-functions shows that a Grand Unification scenario can be reached only in the MSSM framework.

Therefore, with the realization of this work we have shown that supersymmetry can be one way towards the Grand Unification of the three fundamental interactions that are part of the SM. The Grand Unification theories allow us to embed these three interactions and to understand them as a more fundamental interaction, opening the paradigm of the *Theory of Everything*, in which the gravitational interaction would also be unified. Lastly, althought the SM has be proven with the largest precision, it has unanswered questions that keep supersymmetry as a candidate to solve experimental and theoretical problems of the SM.

The code used in this work can be found in the following link: `https://github.com/EduardoTF/Solution-Of-Coupled-beta-Functions-in-Python`.

Acknowledgments

This research was supported in part by COST Action CA16201 (PARTICLEFACE), MCIN/AEI/10.13039/501100011033 Grant No. PID2020-114473GB-I00, PROFAPI 2022 Grant No. PRO_A1_024 (Universidad Autónoma de Sinaloa) and by CONACyT through the Project No. A1-S-33202 (Ciencia Básica), No. 320856 (Paradigmas y Controversias de la Ciencia 2022), Ciencia de Frontera 2021-2042 and Sistema Nacional de Investigadores.

References

[1] I. Newton, Philosophiæ naturalis principia mathematica (Streater, J., & Royal Society, Great Britain, 1687)

[2] B. P. Abbott *et al.* [LIGO Scientific and Virgo], Phys. Rev. Lett. **116**, no.6, 061102 (2016) doi:10.1103/PhysRevLett.116.061102 [arXiv:1602.03837 [gr-qc]].

[3] `https://web.archive.org/web/20070713140711/http://pdg.web.cern.ch/pdg/particleadventure/spanish/interactions_charts.html`

[4] M. Gell-Mann, Phys. Lett. **8** (1964), 214-215 doi:10.1016/S0031-9163(64)92001-3

[5] G. Zweig, CERN-TH-401.

[6] G. Zweig, CERN-TH-412.

[7] J. Cobián, El Modelo Estándar de la Física de Partículas (Sociedad Nuclear Española,2018)

[8] G. Aad *et al.* [ATLAS], Phys. Lett. B **716** (2012), 1-29 doi:10.1016/j.physletb.2012.08.020 [arXiv:1207.7214 [hep-ex]].

[9] S. Chatrchyan *et al.* [CMS], Phys. Lett. B **716** (2012), 30-61 doi:10.1016/j.physletb.2012.08.021 [arXiv:1207.7235 [hep-ex]].

[10] P. A. Zyla *et al.* [Particle Data Group], PTEP **2020**, no.8, 083C01 (2020) doi:10.1093/ptep/ptaa104

[11] M. A. Moreira, Revista Brasileira de Ensino de Física, 31(1), 1306.1–1306.11. doi:10.1590/s1806-11172009000100006

[12] P.A. Tipler and R.A. Llewellyn, Modern Physics (W.H. Freeman and Company, 2012)

[13] A. Sommerfeld, Zur Quantentheorie der Spektrallinien. Annalen Der Physik, 356(17), 1–94. doi:10.1002/andp.19163561702

[14] M. E. Machacek and M. T. Vaughn, Nucl. Phys. B **222** (1983), 83-103 doi:10.1016/0550-3213(83)90610-7

[15] S. Weinberg, Phys. Rev. Lett. **19** (1967), 1264-1266 doi:10.1103/PhysRevLett.19.1264

[16] A. Salam and J. C. Ward, Phys. Lett. **13** (1964), 168-171 doi:10.1016/0031-9163(64)90711-5

[17] S. L. Glashow, Nucl. Phys. **10** (1959), 107-117 doi:10.1016/0029-5582(59)90196-8

[18] J.W. Rohlf, Modern Physics from α to Z^0 (John Wiley & Sons, Inc,1994)

[19] S. P. Martin, Adv. Ser. Direct. High Energy Phys. **18** (1998), 1-98 doi:10.1142/9789812839657_0001 [arXiv:hep-ph/9709356 [hep-ph]].

[20] S. P. Martin and M. T. Vaughn, Phys. Rev. D **50** (1994), 2282 [erratum: Phys. Rev. D **78** (2008), 039903] doi:10.1103/PhysRevD.50.2282 [arXiv:hep-ph/9311340 [hep-ph]].

[21] A. Iserles, A First Course in the Numerical Analysis of Differential Equations (Cambridge University Press,1996)

[22] J. Kiusalaas, Numerical methods in engineering with Python 3 (Cambridge university press, 2013).

[23] P. A. Zyla *et al.* [Particle Data Group], PTEP **2020** (2020) no.8, 083C01 doi:10.1093/ptep/ptaa104

[24] A. Abada *et al.* [FCC], Eur. Phys. J. ST **228**, no.4, 755-1107 (2019) doi:10.1140/epjst/e2019-900087-0

[25] A. Abada *et al.* [FCC], Eur. Phys. J. ST **228**, no.5, 1109-1382 (2019) doi:10.1140/epjst/e2019-900088-6

[26] A. Abada *et al.* [FCC], Eur. Phys. J. ST **228**, no.2, 261-623 (2019) doi:10.1140/epjst/e2019-900045-4

[27] A. Abada *et al.* [FCC], Eur. Phys. J. C **79**, no.6, 474 (2019) doi:10.1140/epjc/s10052-019-6904-3